Electrical Power and Energy Systems 131 (2021) 107128

Contents lists available at ScienceDirect

International Journal of Electrical Power and Energy Systems

journal homepage: www.elsevier.com/locate/ijepes

# A metaheuristic optimization model for the inter-array layout planning of floating offshore wind farms

Markus Lerch [a,*], Mikel De-Prada-Gil [b], Climent Molins [a]

[a] UPC Universitat Politècnica de Catalunya, Department of Civil and Environmental Engineering, Jordi Girona 1-3, Barcelona 08034, Spain
[b] General Electric Renewable Energy, Roc Boronat 78, Barcelona 08005, Spain

ARTICLE INFO

*Keywords:*
Electrical layout
Inter-array cable routing
Particle swarm optimization
Floating offshore wind farm
Dynamic and static power cables

ABSTRACT

This paper presents an adapted particle swarm optimization model for the electrical layout planning of floating offshore wind farms (FOWFs). A comprehensive model is considered by taking into account the entire wind turbine connection possibilities as well as stochastic wind speed and wind direction and the computation of the wake effect within the wind farm. Furthermore, dynamic power cables used for the connection of floating offshore wind turbines are considered as well as their respective acquisition and installation costs. The reliability assessment of the electrical components and the influence on the energy generation are also taken into account. The developed optimization model is validated in this paper at first against a reference model developed by Banzo et al. Then the model is applied on a 500 MW FOWF case. The optimized collection grid results in a decrease of 4.5% of the total costs and a reduction of the energy losses by 6.4% compared to the existing layout of the FOWF. Finally, the use of either solely dynamic power cables or a combination of static and dynamic cables is studied. The findings show that for this particular case the use of solely dynamic power cables is favorable due to the avoidance of cost-intensive submarine joints and additional installation activities.

## 1. Introduction

The increasing demand for clean energy to reduce carbon emissions and reach defined energy targets based on renewable energy sources has been one of the key drivers of the formation and rapid growth of the offshore wind industry in Europe. As the wind speeds tend to be faster and steadier offshore, wind farms at sea can reach higher capacity factors compared to their onshore counterparts. Furthermore, fewer restrictions regarding land use, visual impact, and noise favors the application of this technology [1]. It is expected that the offshore wind industry will continue growing and expand worldwide [2]. However, most of today's offshore wind farms use bottom-fixed foundations that limit their feasible application to shallow water depths. Floating substructures for offshore wind turbines are a suitable solution to harness the full potential of offshore wind as they have less constraints to water depths and soil conditions and can be applied from shallow to deep waters [3].

It is estimated that 80% of all the offshore wind resource in Europe is located in water depths greater than 60 m. Moreover, floating offshore wind turbines (FOWTs) allow countries such as Japan, Spain, Portugal and Norway that lack of shallow water sites to construct offshore wind farms and enter the offshore wind market [4]. Recently, WindEurope has outlined in its policy blueprint [5] the large potential of floating offshore wind and the ability to reach a levelized cost of energy of about 40€/MWh to 60€/MWh for commercial floating offshore wind farms (FOWFs) by 2030. However, this is only achievable by significant cost reductions along the whole supply chain.

The cost of the electrical system of bottom-fixed offshore wind farms (BOWFs) can take up to 15% to 30% of the total investment in which the cost of cables takes a large portion [6]. For FOWFs the costs might be even higher since new technologies and installations procedures are applied. For instance, dynamic power cables are used that include additional buoyancy components and joints. Furthermore, floating substations are needed, which represent a crucial component of the electrical system. Besides that, commercial scale FOWFs will likely include wind turbines with power ratings ranging from 6 MW to 10 MW or more, which require dynamic power cables with higher voltage levels. Hence, it is desirable to optimize the electrical layout to obtain the most cost-effective solution. The offshore substation location and the export cable are also considered. The electrical layout impacts both the energy yield and the costs. The energy yield of the wind farm takes into account the energy generation by each wind turbine and the losses

* Corresponding author.
*E-mail address:* markus.j.lerch@gmail.com (M. Lerch).

https://doi.org/10.1016/j.ijepes.2021.107128
Received 28 January 2020; Received in revised form 22 October 2020; Accepted 18 April 2021
Available online 6 May 2021

appearing in the power cables. The energy generation is based on the wind speed available at the location and is impacted by the wake effect occurring within the wind farm. The costs are a function of the cable length and the configuration as well as the installation procedure [7].

The optimization methods applied in literature to this kind of problem can be classified in deterministic and metaheuristic methods. Mixed integer programming, as a classic deterministic optimization method, has been used in [8–16]. A common approach for deterministic methods is to solve the cable routing optimization problem as a minimum spanning tree. However, it has been found that the computational time increases significantly with the amount of turbines. The problem becomes essentially complex to unsolvable as more turbines and, therefore, potential connections are added [7]. Besides that, as the power loss calculation is based on a nonlinear equation of the current flowing in the cable, the problem becomes more difficult to solve by, for instance, a mixed integer linear programming method [17]. Power losses have been included in [12–14], however, in order to solve the problem for a larger wind farm constraints have been added to reduce the complexity of problem. For instance, in [14] the amount of possible cables entering a turbine has been reduced to one and in [12] the connection is restricted to the subsequent turbine in a row. Moreover, the stochastic characteristics of wind speed and direction are not taken into account in [12]. Due to the complexity, a number of studies have investigated the use of heuristic methods [18–22] or a combination [7,17,23,24]. The authors have opted to a model that may not find a proven optimal solution but a feasible one in a reasonable time with less constraints [7].

In [19] a genetic algorithm (GA) has been used to optimize the electrical system of an offshore wind farm considering the capital cost of the cables, energy production and reliability of system components due to failures. However, three predefined collection grid layouts have been considered to reduce the complexity and the wake effect is not taken into account. In [18] a particle swarm optimization (PSO) model has been applied as well as a single wake model considered. However, the fluctuations in wind speed and wind direction have not been taken into account as well as no installation cost and reliability. In [25] an adaptive PSO algorithm has been applied that addresses the stochastic characteristics of wind speed and direction. PSO possesses many similarities with evolutionary optimization methods such as GA but differs in the optimization algorithm, which is based on swarm intelligence. The implementation of PSO tends to be simpler with less parameters to adjust [26]. Investigations have also been performed on the joint optimization of both cable layout and wind turbine positions as for instance in [27,28] by applying either a mixed integer particle swarm optimization algorithm or a multi-objective random search.

The previous work has addressed mainly the optimization of the electrical layout of BOWFs. The objective of this paper is to solve the electrical layout problem of a FOWF by applying an adapted particle swarm optimization model. The complexity is increased by considering the stochasticity of wind speed and wind direction and taking into account the entire wind turbine connection possibilities. Besides that, a comprehensive wake model is included. Furthermore, dynamic power cables used for the connection of FOWTs are considered as well as their respective acquisition and installation costs. The reliability assessment of the electrical components and the influence on the energy generation are also taken into account. The paper is organized as follows. Section 2 presents the models considered for the FOWF. The developed optimization algorithm is described in Section 3 and the optimization function is defined in Section 4. The application cases of the model are presented in Section 5 and the conclusions of the paper are provided in Section 6.

## 2. Floating offshore wind farm model

In this section, the FOWF model is described including the electrical system, wake effect model and the computation of the energy losses in the power cables. Furthermore, the reliability assessment due to failures is outlined.

### 2.1. Electrical system

The electrical system of an offshore wind farm includes the inter-array cables, offshore substation and the export cable as illustrated in Fig. 1. Inter-array cables are used to connect the FOWTs and to transmit the generated energy to the offshore substation. They are typically three-core copper conductors with steel wire armored and insolation components. The nominal operating voltage of the inter-array cable system of current offshore wind farms is typically 33 kV. However, with the development of larger wind turbines with higher power ratings, higher voltage levels are required such as 66 kV [29]. The offshore substation is equipped with a transformer to increase the medium voltage of the collection grid to high voltage in order to reduce losses during transmission to the shore. In a floating offshore wind farm the topside of the substation is also mounted on a floating substructure. The export cable transmits the collected energy from the offshore to the onshore substation and may operate with HVAC or HVDC technology depending on the distance and power rating of the wind farm [29]. While power cables for BOWFs are buried under the seabed and connected to the structure by a J-tube or J-tubeless interface, the cables for FOWTs have a dynamic section that moves with the floating substructure [30].

The dynamic cable requires a high level of flexibility and mechanical strength in order to withstand the combined impacts of waves, currents, seabed interactions and floater motions [29]. Potential configurations of dynamic cables can be derived from offshore risers used in the oil and gas industry and include, e.g. lazy wave, steep wave, lazy S among

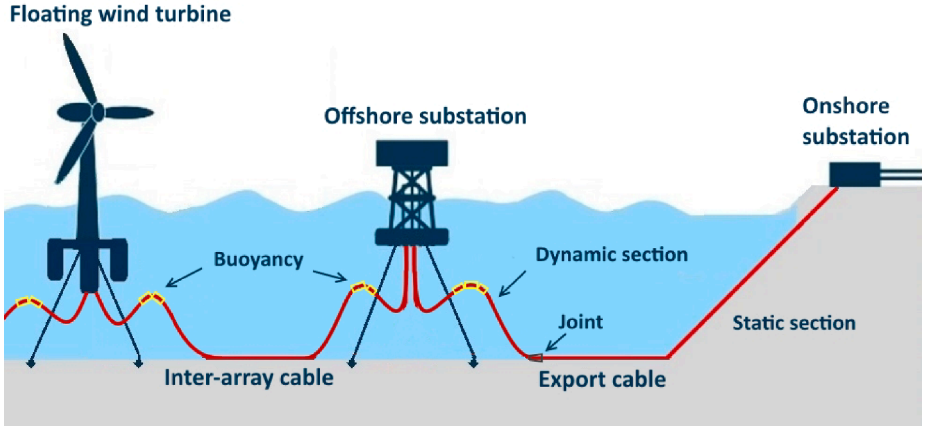


**Fig. 1.** Electrical system of a floating offshore wind farm.

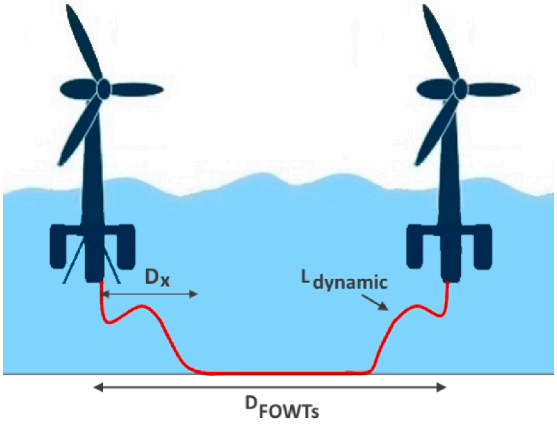


**Fig. 2.** Power cable length illustration.

others [31]. The lazy wave has been the preferred configuration in demonstration projects such as Hywind Scotland [32] and Fukushima [33] and is shown in Fig. 1.

The lazy wave configuration applies buoyancy modules to reduce the load on the cable by providing mid-water suspension. In this way, the substructure motion is decoupled from the cable touchdown at the seabed and the dynamic responses and tension of the cable are reduced [29]. A single dynamic cable can be used for a FOWT connection or a combination of static and dynamic cables. Static cables are lower priced, but a submarine joint is required to connect both cable types. Section 5.3 of this paper analyzes and compares the two connection options. The optimization of the electrical layout of FOWTs gains additional importance because the length of a power cable is increased due to the dynamic cable section, spatial requirements of the mooring system and the offset of the floating substructure. For bottom-fixed wind turbines a common approach in literature is to simply calculate the geometric distance between wind turbines without considering the water depth [12,18,34]. The length of the power cable used for the connection of FOWTs can be obtained by the following equation, which is based on a collaboration with the floating wind industry.

$$L_{cable} = 1.05*D_{FOWTs} + 2*(L_{dynamic} - D_x), \tag{1}$$

where $D_{FOWTs}$ is the distance between FOWTs, $L_{dynamic}$ represents the length of the dynamic cable section and $D_x$ accounts for the horizontal distance from the substructure to the touchdown point at the seabed. The equation considers a 5% increase of the static part of the cable to allow for routing around the mooring system anchors, as based on discussion with the industry. For the sack of clarity, the variables are illustrated in Fig. 2.

The length of the dynamic cable part can be determined by a segmentation into three catenary lines and calculating the arc length of each catenary assuming the curvature as a hyperbolic cosine function. The numerical modeling of deep sea risers has been widely discussed in marine engineering literature. For the computation of the lazy wave catenary riser length one may refer to [35].

### 2.2. Wake model

A comprehensive wake model has been included in the optimization model to calculate the wind speed for the power generation calculation at each FOWT. The model considers single, partial and multiple wake effects among turbines. Besides that, it takes into account the wind direction of the free-stream wind speed. It is based on the wake concept developed by Jensen [36]. Furthermore, the global momentum conservation in the wake downstream of the wind turbine is considered as well as a linear expansion of the wake downstream. However, turbulent behavior caused by wakes is neglected. A detailed description of the model is provided in [37,38].

### 2.3. Energy loss computation

The power generated by a wind turbine can be calculated as follows

$$P_{gen} = \frac{1}{2}\rho_a A_{rotor} C_p(v_{wind}) v_{wind}^3, \tag{2}$$

where $A_{rotor}$ accounts for the rotor swept area and $\rho_a$ for the density of air. $C_p$ is the power coefficient and $v_{wind}$ represents the wind speed at hub height. The power loss in any power cable of the FOWF can be determined by

$$P_{loss} = 3\left(\frac{P_{gen} + P_{trans}}{\sqrt{3}*U}\right)^2 * R_{cable} * L_{cable}, \tag{3}$$

where $P_{gen}$ is the power generated by the FOWT from which the cables exists. $P_{trans}$ represents the power that has been transmitted to this FOWT from other wind turbines. U is the voltage applied, for example, medium voltage for inter-array cables and high voltage for the export cable. The resistance of the power cable is represented by $R_{cable}$ and $L_{cable}$ defines the length of the cable. The energy loss can, finally, be obtained by

$$E_{loss} = \sum_{v_{wind}=v_{in}}^{v_{out}} \sum_{\alpha=0°}^{360°} P_{loss} * H_{ws} * H_{wd} * T, \tag{4}$$

where $v_{in}$ and $v_{out}$ are the cut-in and cut-out wind speed, respectively. $T$ is the expected lifetime of the FOWF. Wind speed and wind direction are included as stochastic variables. The occurrence probabilities of wind speed and wind direction are defined by $H_{ws}$ and $H_{wd}$, respectively. The total energy losses are obtained as the sum of energy losses according to different wind speeds and wind directions $(\alpha)$.

### 2.4. Reliability assessment

Certain components of the electrical infrastructure of an offshore wind farm may fail and interrupt partially or completely the energy generation. These unexpected losses due to unforeseen equipment failures are very important in offshore wind farms since severe weather conditions can lead to a long downtime for maintenance and implying significant undesired associated costs [38]. The resulting energy losses are defined as expected energy not supplied (EENS) and the calculation of these losses is based on reliability multi-state models as explained in detail in [39]. The models consider that each component has several states of service with a respective probability of occurrence. In this study, the reliability assessment is carried out for the inter-array cables connecting to the offshore substation, the export cable as well as the transformers in the offshore substation. The states of service are available and unavailable. Furthermore, the N-1 criterion is considered, which defines that at most one component can be unavailable at a time [12]. The probability of being available $A$ is given by

$$A = \frac{MTBF}{MTBF + MTTR} = \frac{1}{1 + \lambda * MTTR} = \frac{\mu}{\mu + \lambda} \tag{5}$$

where $MTBF$ is the mean time between failure and $MTTR$ represents the mean time to repair with $MTBF{=}\lambda^{-1}$ and $MTTR{=}\mu^{-1}$. The failure rate of a component is defined by $\lambda$ and the repair rate is $\mu$ [39,40]. Consequently, the unavailability probability $U$ is expressed as $U = 1\text{-}A$ and the EENS can be obtained as

$$EENS = \sum_{k=1}^{n} P_k^{cons} * U_k * T, \tag{6}$$

where $P_k^{cons}$ is the power constrained or not delivered in the electrical component $k$ (i.e., power cable or substation transformer) due to a failure. The number of electrical components is defined by $n$ [38].

Likewise the calculation of EENS considers the unavailability, the computation of the energy losses takes into account the availability of the components.

## 3. Numerical optimization model

### 3.1. Particle swarm optimization algorithm

PSO is a population-based metaheuristic optimization algorithm that was chosen due to its simplicity and high computational efficiency in solving non-linear complex problems [23]. In PSO, a possible solution is defined as a particle and is randomly initialized at the beginning. Each particle has its own position vector $x_j = (x_{j1}, x_{j2}, \ldots, x_{jd})$ and velocity vector $v_j = (v_{j1}, v_{j2}, .., v_{jd})$, where $j$ refers to the number of particles and $d$ to the amount of dimensions [41]. A set of particles is called population and moves around in a multi-dimensional search space. The velocity and position of the particles are updated every iteration $k$ according to Eqs. 7 and 8 in order to move the particles through the search space to find new and better solutions. Similar to how a bird of a swarm reconfigures its behavior based on its own experience and the experience of the rest of the birds, each particle updates its position based on its personal best solution *Pbest* found so far, the global best solution *Gbest* found by all particles and according to its velocity of the subsequent iteration $v_j^{k+1}$ [41].

$$v_j^{k+1} = w^k * v_j^k + c_1 * r_1 * (Pbest_j^k - x_j^k) + c_2 * r_2 * (Gbest_j^k - x_j^k) \quad (7)$$

$$x_j^{k+1} = x_j^k + v_j^{k+1} \quad (8)$$

$w^k$ represents the inertia weight. $c_1$ and $c_2$ are positive constants with the value 2 and $r_1$ and $r_2$ are randomly distributed numbers in the range [0,1] [42]. The first term of Eq. 7 is called inertia and ensures that the particle moves in its path and does not change too abruptly. The second represents the memory of a particle and ensures that it moves towards its personal best solution (*Pbest*). The last term includes the cooperation and attracts the particle to a global best solution (*Gbest*), which is the one found by all particles [41]. The inertia weight changes with the iterations and can be determined as follows

$$w^k = w_{max} - \frac{w_{max} - w_{min}}{k_{max}} * k, \quad (9)$$

where $w_{max}$ and $w_{min}$ are the maximum and minimum inertia coefficients and $k_{max}$ represents the maximum number of iterations [43]. The PSO algorithm updates within an iteration loop the particles position, velocity and *Pbest* as well as *Gbest* until convergence is obtained or a maximum number of iterations is reached [34].

**Table 1**
Exemplary illustration of a matrix solution.

| Turbine out | Turbine/OSS in | Cable type | Maximal power (MW) |
|---|---|---|---|
| 1 | 2 | 1 | 3 |
| 2 | 5 | 2 | 6 |
| 3 | 4 | 1 | 3 |
| 4 | 5 | 2 | 6 |

### 3.2. Model implementation

The optimization model, based on PSO theory, has been implemented using MATLAB programming language and has been adapted in order to solve the collection grid optimization problem of this paper. The algorithm is illustrated in Fig. 4. The developed PSO model initializes with the definition of the main parameters and information about the wind farm layout such as the location of the wind turbines. Afterwards, an initial population is created consisting of particles with a three-dimensional position matrix.

$$x(a, 4, b), a \in \{1, 2, \ldots, N_{wt}\}, b \in \{1, 2, \ldots, j\}, \quad (10)$$

where $N_{wt}$ is the number of FOWTs and j the number of particles. The particles represent potential solutions, which have been created initially based on an iterative and stochastic process. For a particle the connection of wind turbines is determined by the distance between turbines and an associated probability distribution. This means for a specific turbine the probability of connecting to another wind turbine in the vicinity is higher than to a distant one. The allocation of the wind turbine connections is realized by using the MATLAB function Randsample. The sampling weights of the function considers the connection probabilities based on the distance between turbines.

In the second dimension of the position matrix four types of essential information are saved, namely the number of the turbine from which the power cable leaves, the number of the turbine or substation to which the cable is being connected, the type of cable used for a connection and the maximal power transmitted. The maximal power transmitted refers to the power at the inlet of the cable, which includes the rated power of the wind turbine plus the rated power transmitted to that wind turbine from previous connections. For the sake of clarity, Table 1 represents the matrix solution for a possible cabling connection for the wind farm illustrated in Fig. 3.

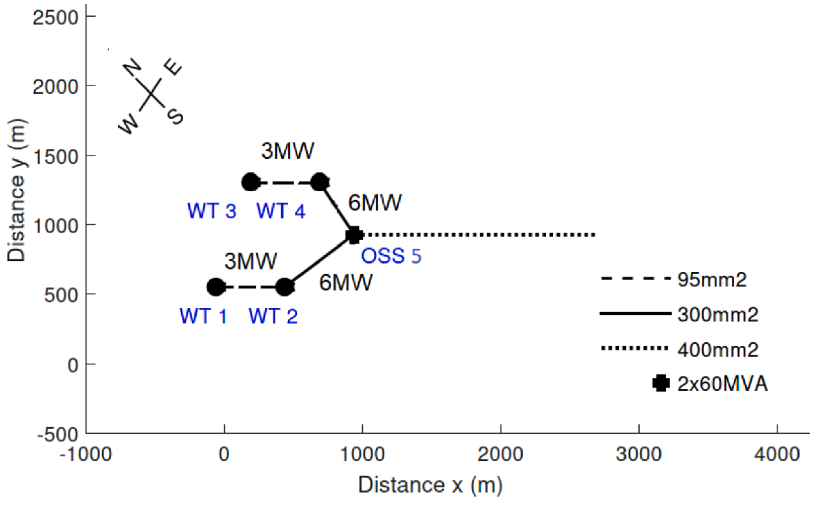


**Fig. 3.** Wind farm connection example.

After the initialization, each particle is checked if it provides a feasible solution to the problem by complying with a set of pre-defined constraints. In case a particle does not comply with a specific constraint, the model reallocates the connection of the FOWTs until the constraint is satisfied. The constraints presented in Section 4.2 are included in the optimization model. When the feasibility of all particles is ensured, the population is searched for the best solution. This can be mathematically described by the minimization of a function, called objective function. This subroutine computes the costs of each particle's solution and determines the one with the lowest total cost, which is then proposed as the initial *Pbest* and *Gbest*. In the next step, the PSO algorithm updates the position and velocity of all particles according to Eqs. 7 and 8 and enters into a loop until a maximum number of iterations is reached. At each iteration the feasibility of the particles is checked as well as *Pbest* and *Gbest* updated by using the objective function.

## 4. Problem statement

### 4.1. Objective problem

The objective is to minimize the cost of the electrical layout considering the cost of acquisition $C_{acquisition}$, the installation cost $C_{installation}$ as well as the costs associated to the energy losses in the cables $C_{loss}$ and the cost of EENS $C_{EENS}$ as shown in Fig. 4.

The objective of this optimization problem can be stated for a single particle as follows.

$$min(C_{acquisition} + C_{installation} + C_{loss} + C_{EENS}) \tag{11}$$

The acquisition cost takes into account the initial investment cost for the inter-array and export power cables as well as the transformer in the offshore substation. Furthermore, amortization is included considering the expected lifetime $T$ of the FOWF as described by the following equation.

$$C_{acquisition} = \left( \sum_{1}^{N_{iac}} (C_{iac} * L_{iac} + C_{aux}) + \sum_{1}^{N_{exc}} (C_{exc} * L_{exc} + C_{aux}) + \sum_{1}^{N_t} C_t \right) * \left( T \frac{i(1+i)^T}{(1+i)^T - 1} \right) \tag{12}$$

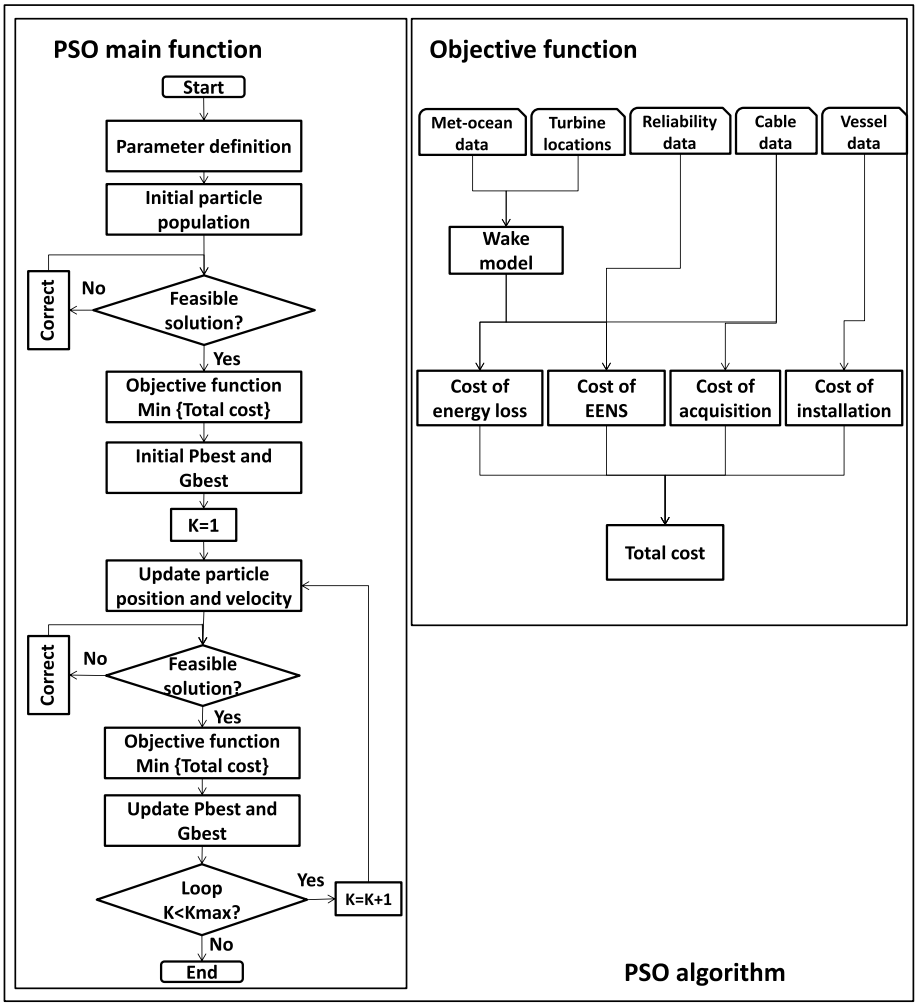


**Fig. 4.** PSO algorithm applied.

where $C_{iac}$ represents the cost per meter of the inter-array cables and $L_{iac}$ the length of the cables used to connect between the FOWTs and the offshore substation. Likewise, $C_{exc}$ defines the cost of the export cable and $L_{exc}$ the length of the export cable. The dynamic power cable requires auxiliary equipment such as buoyancies, bend stiffners and connectors, which cost is taken into account by $C_{aux}$. The cost of the transformer is given by $C_t$. The number of inter-array, export cables and transformers are defined by $N_{iac}$, $N_{exc}$ and $N_t$, respectively. The interest rate used for the calculation of the amortization is defined by $i$. The installation cost includes the cost for installing the power cables and is obtained as

$$C_{installation} = \left( (\sum_{1}^{N_{iac}} L_{iac} + \sum_{1}^{N_{exc}} L_{exc}) * C_{vessel} * r_{instal} + C_{Mob/Demob} \right) * \left( T \frac{i(1+i)^T}{(1+i)^T - 1} \right), \quad (13)$$

where $C_{vessel}$ is the day rate of the cable laying vessel and $r_{instal}$ represents the installation rate in days per meter. The mobilization and demobilization costs of the vessel are defined by a single fixed rate $C_{Mob/Demob}$.

The cost associated to the energy losses in the cables can be determined by

$$C_{loss} = (\sum_{1}^{N_{iac}} Eloss_{iac} + \sum_{1}^{N_{exc}} Eloss_{exc}) * C_{energy}, \quad (14)$$

where $Eloss_{iac}$ and $Eloss_{exc}$ are the energy losses in the inter-array and export cables, respectively. $N_{iac}$ and $N_{exc}$ are the number of inter-array and export cables. The total cost of energy losses is obtained as the sum of energy losses multiplied by the cost per unit of energy $C_{energy}$. The cost of EENS can be obtained as follows

$$C_{EENS} = T \sum_{k=1}^{n} P_k^{cons} * U_k * C_{energy}. \quad (15)$$

### 4.2. Constraints

The optimization model includes several constraints that have to be satisfied by all particles in order to count as a suitable solution.

- The energy leaving a turbine must be supported by a single cable.
- A maximum of one cable can be placed between two turbines.
- The crossing of power cables is not allowed. For more information on cable crossing and implementation solutions one may refer to [44].
- The building of a ring connection is not allowed. A ring is a connection between several FOWTs that does not end in a connection to the offshore substation.
- The power transmitted by a cable cannot exceed the capacity of the installed cable.

## 5. Application

### 5.1. Validation case

At first, the developed optimization model is validated against an existing model used in [12]. The electrical layout of the Barrow BOWF is optimized in [12] by the use of a mixed integer quadratic constraint programming (MIQCP) method. Several constraints and restrictions have been included in order to reduce the complexity of the problem. However, these constraints cause the solution to be less realistic. For instance, cable crossing is allowed, which is not recommended in practice due to potential cable damages [17]. Furthermore, wake effect as well as wind direction are not considered and the range of wind speeds is reduced to 5 scenarios with corresponding power generations. Besides that, the wind turbine connection possibilities have been restricted to the adjacent wind turbine of its row and no installation costs are taken into account. In order to validate and compare the developed PSO model, a simplified version is created containing the before mentioned constraints. At first, the simplified model is used to solve the optimization problem and the results are compared with the reference. Then, the full PSO model is applied to search for a more realistic solution. The Barrow BOWF consists of 30 wind turbines with each having a rated capacity of 3 MW. The collection grid is operated at 33 kV and the export cable transmits the energy at 132 kV. Two possible locations are considered for the offshore substation as shown in Fig. 5. Furthermore, two different transformer capacities (60MVA and 120MVA) are considered with respective costs and availability values. A complete description of the case study and the input data is provided in [12]. In order to match the criteria of the validation case (i.e., two substation locations and two transformer types) the optimization algorithm has been slightly adapted by adding an initial step that assigns randomly to each of the particles a location and a transformer type. The

**Table 2**
Power cable information [12,45].

| | Inter-array 33 kV | | | Export 132 kV | |
|---|---|---|---|---|---|
| Cross section (mm$^2$) | 95 | 120 | 300 | 400 | 630 |
| Power capacity (MW) | 17.9 | 19.43 | 30.29 | 134.89 | 163.47 |
| Resistance (Ω/km) | 0.246 | 0.196 | 0.079 | 0.063 | 0.042 |
| Cable cost (€/m) | 210 | 258 | 354 | 450 | 578 |
| Failure rate (failures/km/year) | 0.149 | 0.149 | 0.149 | 0.179 | 0.179 |
| Repair rate (repairs) | 912.5 | 912.5 | 912.5 | 347.6 | 347.6 |

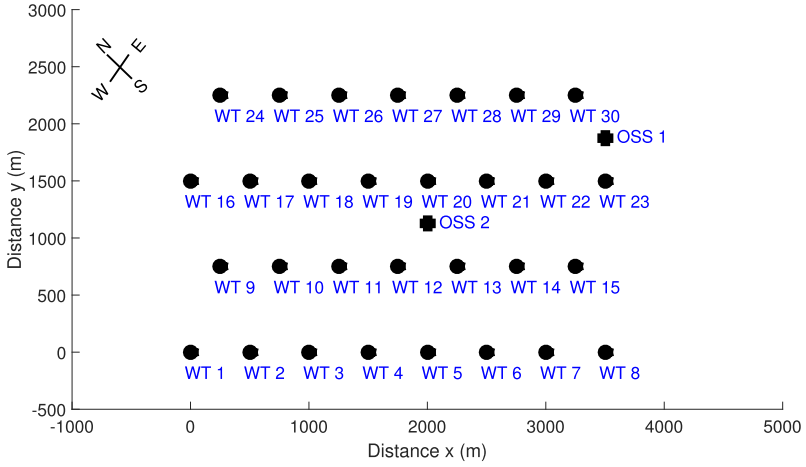


**Fig. 5.** Wind turbine (WT) placements and offshore substation (OSS) locations at Barrow offshore wind farm.

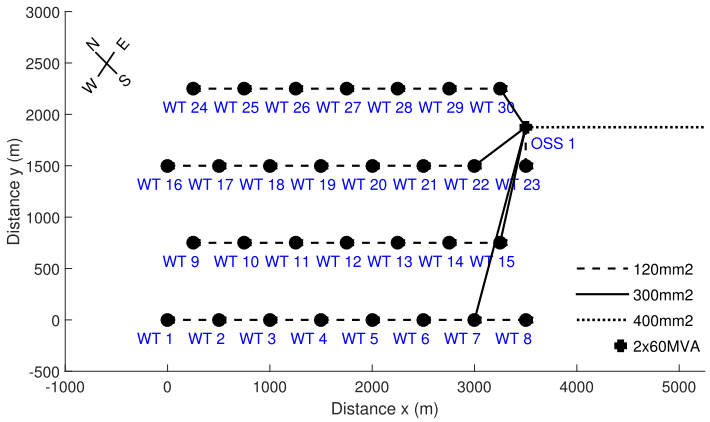


**Fig. 6.** Optimized layout obtained from simplified PSO model.

**Table 3**
Comparison of costs.

| | MIQCP [12] | Simplified PSO | Full PSO |
|---|---|---|---|
| Acquisition cost (M€) | 25.23 | 25.23 | 24.71 |
| Cost of EENS (M€) | 5.29 | 6.39 | 6.36 |
| Cost of energy loss (M€) | 4.09 | 4.19 | 4.17 |
| Total cost (M€) | 34.61 | 35.81 | 35.24 |
| Inter-array length (km) | 17.04 | 17.04 | 16.60 |

model performs then with standard algorithm for the assigned configurations an optimization of the electrical cable layout and provides the cost-optimal solution out of the possible configurations.

The power cable information used as input data for this case study is presented in Table 2.

The simplified PSO model is applied on the Barrow BOWF with the computation of 10 particles and 20 iterations. The cable routing layout obtained from the optimization is presented in Fig. 6. As expected the optimization model has obtained a cable routing where the turbines are connected in a straight row due to the constraint to connect to adjacent wind turbines.

The model has selected offshore substation 1, because costs and energy losses are reduced since less cable length of the more expensive export cable is used. Despite 2 smaller transformers are slightly more expensive than a single larger transformer, the optimization model has chosen to install 2 units of each having 60MVA. This is mainly based on the lower costs of EENS due to failure of the transformers. In case a single large transformer fails, all the power generated by the wind farm would be lost and when a smaller transformer fails still half of the total power can be served. The electrical layout obtained by the simplified PSO model equals the one obtained in [12]. Table 3 presents the costs for this collection grid layout and compares to the results obtained by the MIQCP model of the reference study. The acquisition cost determined by the simplified PSO model matches the value obtained by the MIQCP model. A slight difference is observable in the cost of EENS and the cost of energy losses, which is based on differences in the methodology to calculate the power losses and how the wind speed distribution is considered in the calculation of the energy production. Nevertheless, the PSO model has correctly obtained the optimized electrical layout of the reference study with the same turbine connections and the offshore substation selection. Hence, the PSO model is considered as validated.

The computation time of the simplified PSO model has been 14 s using a Intel Core i5 processor with 2.53 GHz, 4 GB memory and Windows 7 operating system. In comparison, the MIQCP model requires 26 h for the same optimization problem [12]. This demonstrates the high efficiency in solving complex problems by the developed model. As it can be observed in Fig. 6, a cable crosses the connection between wind turbine 14 and 15, which would not be a recommended practice in a real offshore wind farm. Therefore, the full PSO model is applied next on the case study to obtain a more realistic solution. The solution obtained by the full PSO model is presented in Fig. 7.

It is observable that cable crossing is avoided. Furthermore, the model has chosen to use a smaller cable cross section for the first 5 wind turbines in a row, which allows to reduce the cost of cable acquisition by 2% as presented in Table 3. In addition, the optimized layout has provided a reduction of the total length of inter-array cables by about 2.6%, which causes both a decrease in acquisition costs and energy losses.

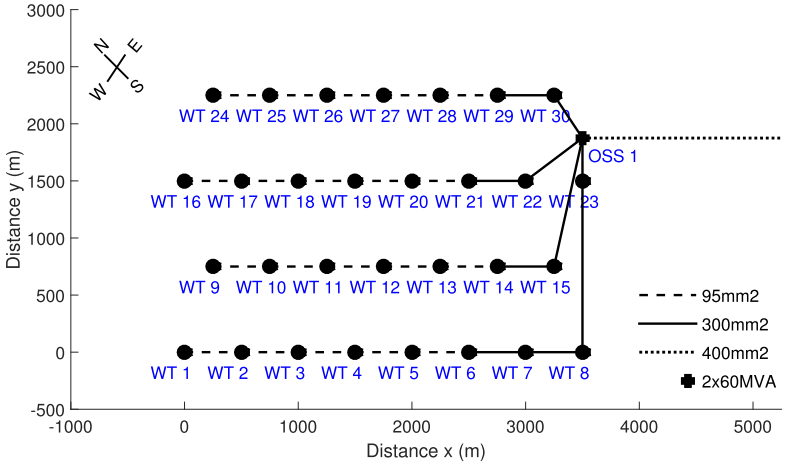


**Fig. 7.** Optimized layout obtained from full PSO model.

### 5.2. Floating offshore wind case study

A 500 MW FOWF has been considered for the application of the optimization model to the case of floating offshore wind. It consists of 50 FOWTs with each having a rated power capacity of 10 MW. The DTU 10 MW reference wind turbine has been considered and related specifications are given in [46]. Golfe de Fos has been chosen as offshore site. It is located in the south of France in the Mediterranean Sea. The reference water depth is about 70 m. The wind rose of the offshore site is presented in Fig. 8 and shows how wind speed and wind direction are distributed at the location.

Further information about the offshore site is provided in [47]. The collection grid of the FOWF is operated at 66 kV and the transmission voltage is 220 kV. Fig. 9 presents the FOWF and the electrical layout, which is based on work performed in the Lifes50+ project [48].

The FOWTs are placed in direction to the prevailing winds. The offshore substation is located to the east of the FOWF. The objective is to optimize the inter-array cable layout by applying the developed PSO model. For this particular case, the offshore substation and export cable are not taken into account in the optimization. The power cable specifications and costs that are considered for the study are presented in Table 4. Additional parameters for the calculation of the installation cost and the reliability are shown in Table 5.

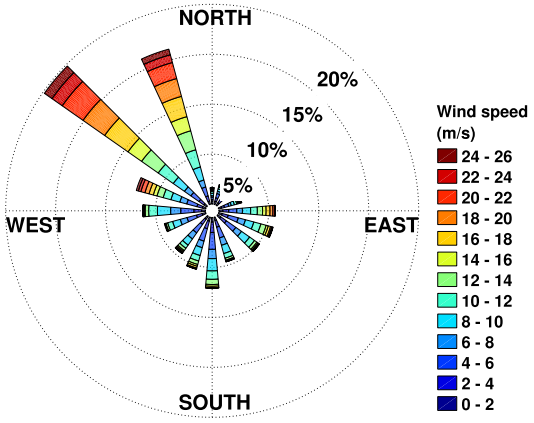


**Fig. 8.** Wind speed and wind direction distribution at Golfe de Fos.

**Table 4**
66 kV inter-array power cable information [49].

| Cross section ($mm^2$) | 95 | 150 | 300 | 400 | 630 | 800 |
|---|---|---|---|---|---|---|
| Power capacity (MW) | 23 | 30 | 40 | 50 | 63 | 71 |
| Resistance (Ω/km) | 0.25 | 0.16 | 0.08 | 0.06 | 0.04 | 0.03 |
| Static cable cost (€/m) | 219 | 300 | 423 | 474 | 554 | 689 |
| Dynamic cable cost (€/m) | 238 | 323 | 456 | 512 | 603 | 748 |
| Buoyancy components (K€) | 59 | 63 | 81 | 90 | 126 | 159 |
| Stiffner and connectors (K€) | 135 | 145 | 172 | 190 | 231 | 262 |

**Table 5**
Installation and reliability parameters [49–51].

| | |
|---|---|
| Installation rate (d/km) | 1.5 |
| Vessel day rate (€/d) | 60,000 |
| Vessel mobilization (€) | 400,000 |
| Vessel demobilization (€) | 400,000 |
| Submarine joints per WT connection (€) | 200,000 |
| 66 kV cable failure rate (failures/km/year) | 0.0094 |
| 66 kV cable mean time to repair (months) | 2 |

The full optimization model is applied on the FOWF case. The number of particles is set to 15 and a total of 40 iterations is considered. The inter-array connection layout obtained from the optimization is presented in Fig. 10.

The optimized collection grid is similar to the Lifes50+ layout but some changes are observable. For instance, the number of FOWTs connected to the offshore substation has decreased from 10 to 8. Furthermore, there exist strings of cables where a higher number of FOWTs are connected. For example, a string of 7 FOWTs exists that requires the use of inter-array cables with larger cross sections up to 800 $mm^2$. Fig. 11 presents the result for the total cost corresponding to each iteration of the optimization model. Furthermore, the results are shown for 5 different runs of the PSO model.

It can be seen from Fig. 11 that the optimization model obtains the final result already after 18 iterations in the first run of the model. Moreover, it can be observed that the model successfully converges to the minimum total cost in each of the performed runs. Table 6 presents the costs and energy losses for the obtained collection grid layout and compares to the Lifes50+ one.

In comparison to the Lifes50+ layout, it can be seen that the total

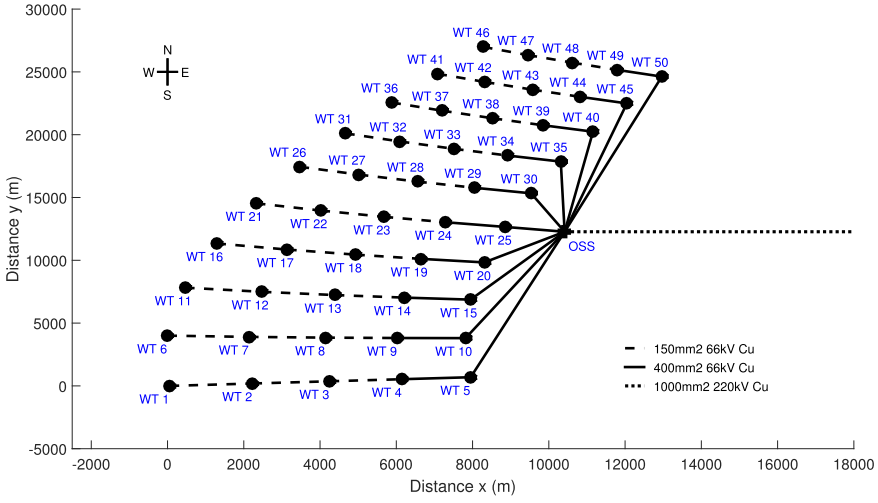


**Fig. 9.** Lifes50+ Golfe de Fos electrical layout [47].

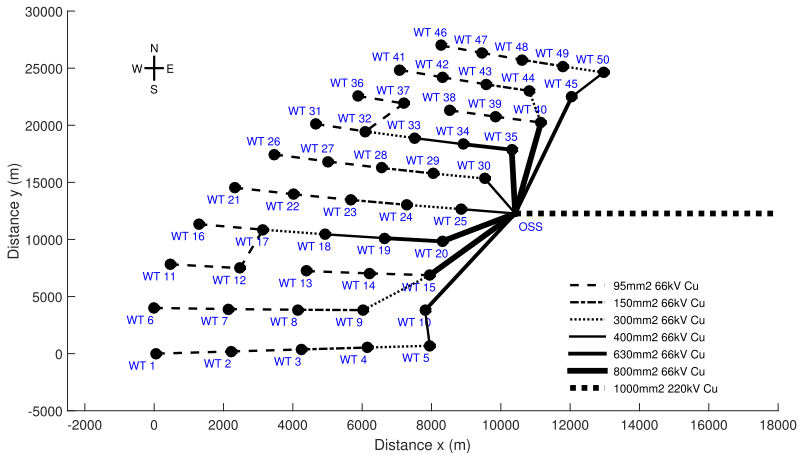


**Fig. 10.** Golfe de Fos optimized collection grid.

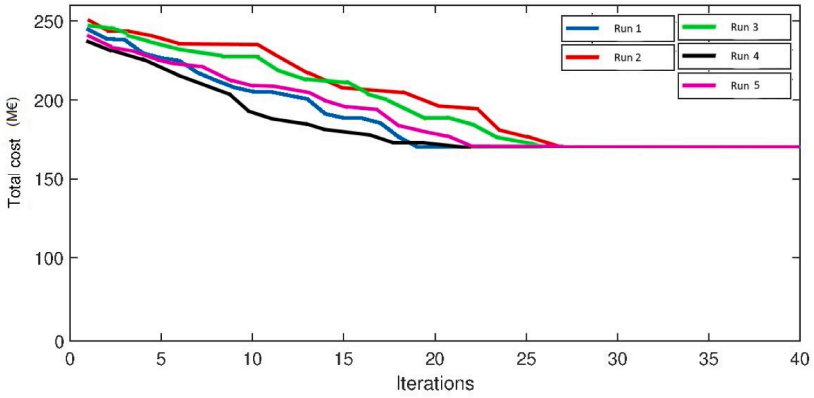


**Fig. 11.** Total cost corresponding to each iteration for optimized collection grid layout.

**Table 6**
Comparison of results for Lifes50+ and optimized collection grid layout.

| | Lifes50+ | Optimized | Difference (%) |
|---|---|---|---|
| Acquisition cost (M€) | 122.75 | 118.17 | −3.73 |
| Installation cost (M€) | 22.82 | 20.85 | −8.63 |
| Cost of energy loss (M€) | 23.90 | 22.39 | −6.32 |
| Cost of EENS (M€) | 8.93 | 8.92 | −0.11 |
| Total cost (M€) | 178.40 | 170.33 | −4.52 |
| Annual energy loss (GWh) | 14.94 | 13.99 | −6.36 |
| Total length of cables (km) | 150.41 | 136.75 | −9.08 |

cost of the inter-array cables has decreased by more than 4.5% and the energy losses by about 6.4% despite the use of more expensive larger cross sections. This is mainly due to the decrease in the total length of the cables since fewer cables are used and less connections to the offshore substation exist. Consequently, the shorter total length of cables has resulted in a decrease in acquisition and installation cost as well as cost of energy losses.

### 5.3. Power cable configuration study

The electrical connection of two FOWTs is made by a combination of a dynamic cable that is designed to withstand the stresses applied by the moving structure and a static cable that is buried in the seabed and transports the power between the turbines [52]. The dynamic cable section has typically a larger outer sheath and increased armor resulting in a higher cost in comparison to the static cable [53]. The connection of the static and dynamic cable can be made through either a permanent factory splice or a submarine joint that enables a separation and re-connection. The submarine joint can be further classified in dry-mate or wet-mate connectors depending on the ability to perform the connection on board of a vessel or under water [50].

Theoretically, the connection of the FOWTs could be done by using only dynamic cables without a static section and by burying a section of the dynamic cable. This would avoid the use of submarine joints, but would lead to higher costs for the cables. In this section, a comparison is made between the two configurations of cable connections. One option is to use only a dynamic power cable for the connection of two FOWTs and burying one section of the cable in the seabed. The second option would be to use the combination of dynamic and static cable with a dry-

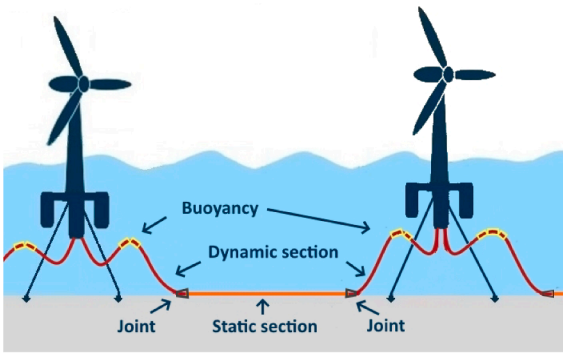


(a) Dynamic with static cable configuration

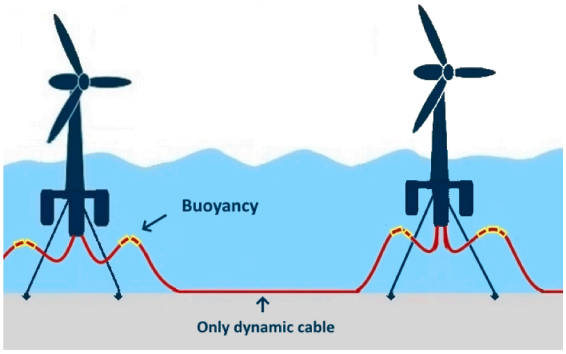


(b) Dynamic cable only configuration

**Fig. 12.** Power cable configurations.

mate connector as submarine joints and where the static section is buried in the seabed. This option has been considered in Section 5.2. Fig. 12 demonstrates the two wind turbine connection configurations.

The cost of cable acquisition and installation differs slightly between two power cable configurations. The cost calculations associated to a single power cable for each configuration (C1 and C2) without taking into account amortization are shown next.

$$C_{acquisition-C1} = C_{static}{}^{*}L_{static} + C_{dynamic}{}^{*}L_{dynamic} + C_{buoy} + C_{stiff} + C_{joint} \quad (16)$$

$$C_{installation-C1} = L_{iac}{}^{*}C_{vessel}{}^{*}r_{instal}{}^{*}1.1 + C_{Mob/Demob} \quad (17)$$

$$C_{acquisition-C2} = C_{dynamic}{}^{*}L_{dynamic} + C_{buoy} + C_{stiff} \quad (18)$$

$$C_{installation-C2} = L_{iac}{}^{*}C_{vessel}{}^{*}r_{instal} + C_{Mob/Demob} \quad (19)$$

$C_{dynamic}$ and $C_{static}$ represent the cost per meter of the dynamic and static cable with the associated length of the cable $L_{dynamic}$ and $L_{static}$, respectively. The cost of the buoyancies required for the dynamic section are defined by $C_{buoy}$ and the cost of bend stiffners and connectors are represented by $C_{stiff}$. The cost of the submarine joints required by cable configuration C1 is defined by $C_{joint}$. Furthermore, as the connection of the static and dynamic cable section is performed offshore, an increase of 10% is taken into account for the installation cost of C1. The optimized collection grid layout obtained in Section 5.2 is considered and the cable configurations C2 is applied and compared to the results of C1 that have been obtained in the previous section. Fig. 13 shows the comparison of the results for both cable configurations. It is observable that the acquisition cost of the cable configuration C2 has decreased despite using solely the slightly more expensive dynamic power cables. This is based on the avoidance of the submarine joints, which are required for cable configuration C1. Furthermore, the installation cost has decreased for C2, because no additional cost for the installation of the submarine joints is required.

The energy losses are not influenced by the type of cable configuration since the same resistance is assumed for both dynamic and static cables. The total cost of the collection grid has decreased by 6.5% considering the use of only dynamic power cables.

## 6. Conclusion

In this paper, an optimization model based on an adapted metaheuristic PSO algorithm has been presented for the electrical layout planning of FOWFs. The model possesses a high complexity by considering the stochasticity of wind speed and wind direction and taking into account the entire wind turbine connection possibilities. Besides that, a comprehensive wake model is included. Furthermore, dynamic power cables used for the connection of FOWTs are considered as well as their respective acquisition and installation costs. The reliability assessment of the electrical components and the influence on the energy generation are also taken into account. The developed PSO model has been applied on different case studies. At first, a validation of the model has been performed by the results obtained of a simplified version of the model to a reference one including the same restrictions and assumptions.

The simplified PSO model has obtained the same electrical layout as the reference model but with a significant reduction in computation time. A slight difference has been observed for the cost of EENS and energy losses, which is based on a different approach for the energy loss calculation. Hence, the model has seen to be validated. Then the full PSO model has been applied with all its functionalities. The model has successfully avoided a cable crossing in the obtained layout and provided an

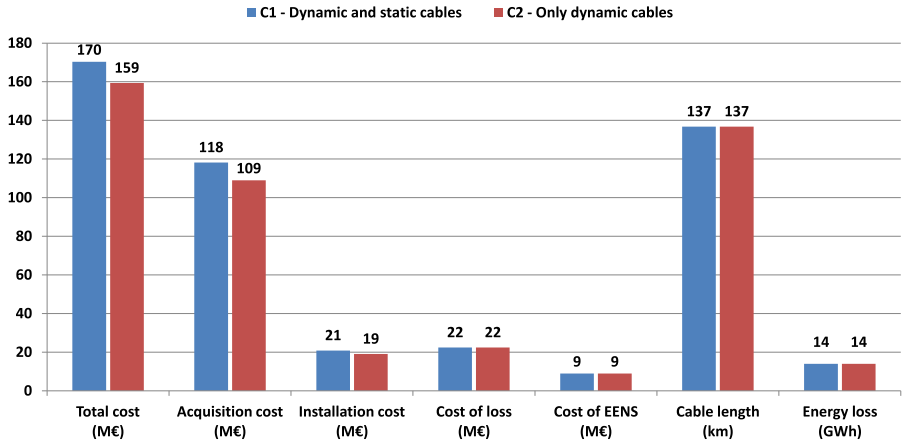


**Fig. 13.** Comparison of inter-array costs and energy losses for different cable configurations.

optimized layout with a shorter total length of cables and a decrease in acquisition costs and energy losses.

The second application case concerned a 500 MW FOWF. The inter-array cable layout has been optimized by applying the full PSO model. The total cost of the inter-array cables could be decreased by 4.5% and the energy losses by 6.4% due to a smaller amount of cables that are used in the optimized layout and fewer connections to the offshore substation. It can be concluded, that the developed optimization model has demonstrated its ability to optimize the electrical layout of FOWFs. As the PSO algorithm by nature does not guarantee to find the optimal solution it involves a risk of premature convergence. However, for the purpose of this study the model has fulfilled its objective by providing an optimized layout in an acceptable time frame.

Finally, different options to connect FOWTs have been studied. The first configuration considered a combination of dynamic and static power cables for the collection grid whereas the second considered only dynamic power cables connected between two FOWTs. It has been shown that for this particular case, considering the predefined wind turbine layout and the specific water depth, the use of solely dynamic power cables results in decreased acquisition costs and installation costs due to the avoidance of cost-intensive submarine joints and additional installation activities.

## CRediT authorship contribution statement

**Markus Lerch:** Conceptualization, Methodology, Software, Writing. **Mikel De-Prada-Gil:** Methodology, Software, Supervision. **Climent Molins:** Supervision.

## Declaration of Competing Interest

The authors declare that they have no known competing financial interests or personal relationships that could have appeared to influence the work reported in this paper.

## Acknowledgments

This work was supported in part by the European Union Horizon 2020 programme under the grant agreement H2020-LCE-2014-1-640741. The authors would like to acknowledge the company IDEOL for providing practical information for the research.

## References

[1] Ng C, Ran L. Offshore wind farms: Technologies, design and operation. 1st ed. Woodhead Publishing; 2016.
[2] Global Wind Energy Council. Global wind report - Annual market update 2017, 2018. p. 1–72.
[3] Atcheson M, Garrad A. Looking back. In: Floating offshore wind energy: the next generation of wind energy. 1st ed. Springer International Publishing Switzerland; 2016. p. 1–20.
[4] WindEurope. Floating offshore wind vision statement, 2017. p. 1–16.
[5] WindEurope. Floating offshore wind energy: A policy blueprint for europe, 2018, p. 1–9.
[6] Ling-Ling H, Ning C, Hongyue Z, Yang F. Optimization of large-scale offshore wind farm electrical collection systems based on improved fcm. IET 2012:1–6.
[7] Pillai A, Chick J, Johanning L, Khorasanchi M, de Laleu V. Offshore wind farm electrical cable layout optimization. Eng Optim 2015;47(12):1689–708.
[8] Fagerfjäll P. Optimizing wind farm layout: more bang for the buck using mixed integer linear programming, Master's thesis, Chalmers University of Technology and Gothenburg University, 2010.
[9] Svendsen HG. Planning tool for clustering and optimised grid connection of offshore wind farms. Energy Procedia 2013;35:297–306.
[10] Lindahl M, Bagger N, Stidsen T, Ahrenfeldt SF, Arana I. Optiarray from dong energy. In: Proceedings 12th Workshop Large-Scale Integration of Wind Power into Power Systems, 2013.
[11] Berzan C, Veeramachaneni K, McDermott J, O'Reilly U-M. Algorithms for cable network design on large-scale wind farms. Massachusetts Inst Technol 2011;144:1–24.
[12] Banzo M, Ramos A. Stochastic optimization model for electric power system planning of offshore wind farms. IEEE Trans Power Syst 2011;26(3):1338–48.
[13] Cerveira A, de Sousa A, Pires ES, Baptista J. Optimal cable design of wind farms: The infrastructure and losses cost minimization case. IEEE Trans Power Syst 2016;31(6):4319–29.
[14] Bauer J, Lysgaard J. The offshore wind farm array cable layout problem: a planar open vehicle routing problem. J Oper Res Soc 2015;66(3):360–8.
[15] Samarakoon H, Shrestha R, Fujiwara O. A mixed integer linear programming model for transmission expansion planning with generation location selection. Int J Electrical Power Energy Syst 2001;23(4):285–93.
[16] Lakhera S, Shanbhag UV, McInerney MK. Approximating electrical distribution networks via mixed-integer nonlinear programming. Int J Electrical Power Energy Syst 2011;33(2):245–57.
[17] Fischetti M, Pisinger D. Optimizing wind farm cable routing considering power losses. Eur J Oper Res 2018;270(3):917–30.
[18] Hou P, Yang G, Hu W, Chen C, Soltani M, Chen Z. Cable connection scheme optimization for offshore wind farm considering wake effect. In: 2018 IEEE Congress on Evolutionary Computation (CEC); 2018. p. 1–8.
[19] Zhao M, Chen Z, Blaabjerg F. Optimisation of electrical system for offshore wind farms via genetic algorithm. IET Renew Power Gener 2009;3(2):205–16.
[20] Gonzalez-Longatt FM, Wall P, Regulski P, Terzija V. Optimal electric network design for a large offshore wind farm based on a modified genetic algorithm approach. IEEE Syst J 2012;6(1):164–72.
[21] Zhao M, Chen Z, Blaabjerg F. Optimization of electrical system for a large dc offshore wind farm by genetic algorithm. In: Proceedings of NORPIE 2004, vol. 37, 2004, p. 1–8.
[22] Dutta S, Overbye T. A clustering based wind farm collector system cable layout design. In: 2011 IEEE Power and Energy Conference at Illinois; 2011. p. 1–6.
[23] Hou P, Hu W, Chen Z. Optimisation for offshore wind farm cable connection layout using adaptive particle swarm optimisation minimum spanning tree method. IET Renew Power Gener 2016;10(5):694–702.
[24] Li DD, He C, Fu Y. Optimization of internal electric connection system of large offshore wind farm with hybrid genetic and immune algorithm. In: 2008 Third International Conference on Electric Utility Deregulation and Restructuring and Power Technologies; 2008. p. 2476–81.
[25] Jin R, Hou P, Yang G, Qi Y, Chen C, Chen Z. Cable routing optimization for offshore wind power plants via wind scenarios considering power loss cost model. Appl Energy 2019;254:113719.
[26] Jones KO. Comparison of genetic algorithm and particle swarm optimization. In: Proceedings of the International Conference on Computer Systems and Technologies; 2005. p. 1–6.
[27] Hou P, Hu W, Soltani M, Chen C, Chen Z. Combined optimization for offshore wind turbine micro siting. Appl Energy 2017;189:271–82.
[28] Feng J, Shen WZ, Xu C. Multi-objective random search algorithm for simultaneously optimizing wind farm layout and number of turbines. In: Journal of Physics: Conference Series, Vol. 753, IOP Publishing, 2016, p. 032011.
[29] Srinil N. Cabling to connect offshore wind turbines to onshore facilities. In: Offshore wind farms: Technologies, design and operation. Woodhead Publishing; 2016. p. 419–40.
[30] Taninoki R, Kazutoshi A, Sukegawa T, Azuma D, Nishikawa M. Dynamic cable system for floating offshore wind power generation. SEI Tech Rev 2017;84(53–58):1–6.
[31] Chandrasekaran S. Dynamic analysis and design of offshore structures. Springer; 2015.
[32] Yttervik R. Hywind Scotland–status and plans. In: EERA DeepWind Conference; 2015. p. 1–26.
[33] Yagihashi K, Tateno Y, Sakakibara H, Manabe H. Dynamic cable installation for fukushima floating offshore wind farm demonstration project. In: Proceedings Jicable 15–International Conference on Insulated Power Cables; 2015. p. 1–28.
[34] Hou P, Hu W, Soltani M, Chen Z. Optimized placement of wind turbines in large-scale offshore wind farm using particle swarm optimization algorithm. IEEE Trans Sustainable Energy 2015;6(4):1272–82.
[35] Li S, Nguyen C. Dynamic response of deepwater lazy-wave catenary riser. In: Deep Offshore Technology International, 2010, p. 1–21.
[36] Jensen NO. A note on wind generator interaction. Risø National Laboratory Roskilde 1983:1–16.
[37] De-Prada-Gil M, Alías CG, Gomis-Bellmunt O, Sumper A. Maximum wind power plant generation by reducing the wake effect. Energy Convers Manage 2015;101:73–84.
[38] De-Prada-Gil M. Design, operation and control of novel electrical concepts for offshore wind power plants, Ph.D. thesis, Universitat Politècnica de Catalunya, 2014.
[39] Lisnianski A, Frenkel I, Ding Y. Multi-state system reliability analysis and optimization for engineers and industrial managers. Springer Science & Business Media; 2010.
[40] Bukowski H. Engineering design handbook maintainability engineering theory and practice. US Army Material Command 1976.
[41] Dauer M, Meyer J, Jaeger J, Bopp T, Krebs R. Epso de algorithm for system-wide protection coordination. In: 2016 Power Systems Computation Conference (PSCC); 2016. p. 1–7.
[42] Abido M. Optimal power flow using particle swarm optimization. Int J Electrical Power Energy Syst 2002;24(7):563–71.
[43] Boubaker S, Djemai M, Manamanni N, M'sahli F. Active modes and switching instants identification for linear switched systems based on discrete particle swarm optimization. Appl Soft Comput 2014;14:482–8.
[44] Fischetti M. Mixed integer programming models and algorithms for wind farm layout and cable routing, Master's thesis, Aalborg University, 2014.

[45] Green J, Bowen A, Fingersh LJ, Wan Y. Electrical collection and transmission systems for offshore wind power. Tech. rep., National Renewable Energy Lab. (NREL), Golden, CO (United States); 2007.
[46] Bak C, Zahle F, Bitsche R, Kim T, Yde A, Henriksen LC, et al. The dtu 10-mw reference wind turbine. In: Danish Wind Power Research, 2013; 2013. p. 1–21.
[47] Gonzalez P, Sánchez G, Llana A, Gonzalez G. Deliverable 1.1 oceanographic and meteorological conditions for the design. Tech. Rep., LIFES50plus, 2015.
[48] LIFES50plus. Innovative floating offshore wind energy, https://lifes50plus.eu. [Accessed December 20, 2018].
[49] LIFES50plus. Data based on information collected in the LIFES50plus project.
[50] Sharkey F, Conlon M, Gaughan K. Practical analysis of key electrical interfaces for wave energy converter arrays. In: International Conference on Ocean Energy 2012 (ICOE), 2012, p. 1–9.
[51] Ferguson A, de Villiers P, Fitzgerald B, Matthiesen J. Benefits in moving the inter-array voltage from 33 kv to 66 kv ac for large offshore wind farms. In: European Wind Energy Association Annual Event Copenhagen, 2012; 2012. p. 1–7.
[52] Arapogianni A, Genachte AB, Ochagavia RM, Vergara JP, Castell D, Tsouroukdissian AR, et al. Deep water; the next step for offshore wind energy. European Wind Energy Association (EWEA); 2013. p. 1–51.
[53] O. Vold, G. Hakon, T. Guttormsen, L. Delp, Hywind scotland pilot park project plan for construction activities 2017, Tech. rep., Statoil (2017).